J. Membrane Biol. 160, 9–25 (1997)

The Journal of
Membrane
Biology

Electrophysiological Characterization of the Flounder Type II Na^+/P_i Cotransporter (NaPi-5) Expressed in *Xenopus laevis* Oocytes

I.C. Forster[1], C.A. Wagner[2], A.E. Busch[2], F. Lang[2], J. Biber[1], N. Hernando[1], H. Murer[1], A. Werner[3]

[1]Institute of Physiology, University of Zurich, Winterthurerstrasse 190, CH-8057 Zürich, Switzerland
[2]Institute of Physiology, Eberhard-Karls University, Tubingen, Germany
[3]Max-Planck-Institute for Molecular Physiology, Dortmund, Germany

Received: 11 March 1997/Revised: 3 June 1997

Abstract: The two electrode voltage clamp technique was used to investigate the steady-state and presteady-state kinetic properties of the type II Na^+/P_i cotransporter NaPi-5, cloned from the kidney of winter flounder (*Pseudopleuronectes americanus*) and expressed in *Xenopus laevis* oocytes. Steady-state P_i-induced currents had a voltage-independent apparent K_m for P_i of 0.03 mM and a Hill coefficient of 1.0 at neutral pH, when superfusing with 96 mM Na^+. The apparent K_m for Na^+ at 1 mM P_i was strongly voltage dependent (increasing from 32 mM at −70 mV to 77 mM at −30 mV) and the Hill coefficient was between 1 and 2, indicating cooperative binding of more than one Na^+ ion. The maximum steady-state current was pH dependent, diminishing by 50% or more for a change from pH 7.8 to pH 6.3. Voltage jumps elicited presteady-state relaxations in the presence of 96 mM Na^+ which were suppressed at saturating P_i (1 mM). Relaxations were absent in non-injected oocytes. Charge was balanced for equal positive and negative steps, saturated at extremes of potential and reversed at the holding potential. Fitting the charge transfer to a Boltzmann relationship typically gave a midpoint voltage ($V_{0.5}$) close to zero and an apparent valency of approximately 0.6. The maximum steady-state transport rate correlated linearly with the maximum P_i-suppressed charge movement, indicating that the relaxations were NaPi-5-specific. The apparent transporter turnover was estimated as 35 sec^{-1}. The voltage dependence of the relaxations was P_i-independent, whereas changes in Na^+ shifted $V_{0.5}$ to −60 mV at 25 mM Na^+. Protons suppressed relaxations but contributed to no detectable charge movement in zero external Na^+. The voltage dependent presteady-state behavior of NaPi-5 could be described by a 3 state model in which the partial reactions involving reorientation of the unloaded carrier and binding of Na^+ contribute to transmembrane charge movement.

Key words: Na^+/P_i cotransporter — Proximal tubule — Voltage clamp — Steady-state — Presteady-state — *Xenopus laevis* oocyte expression

Introduction

The homeostasis of inorganic phosphate (P_i) is maintained via renal glomerular filtration followed by tightly controlled tubular reabsorption. One of the key components involved is a Na^+/P_i cotransport system localized in the brush border membrane of the tubular epithelium which mediates the uptake of P_i against the electrochemical gradient from primary urine into the cell.

The Na^+/P_i cotransporter has been cloned from several mammalian species and it has been expressed and characterized functionally in a variety of eucaryotic systems (*reviewed in:* Biber et al. (1996)). The cloned renal tubular Na^+/P_i cotransport systems which have been classified as type I and type II according to both molecular and functional characteristics, exhibit basic and regulatory properties known to be associated with proximal tubular brush border membrane Na^+/P_i-cotransport (Murer & Biber, 1996). For the type II Na^+/P_i cotransporter, the reported kinetic parameters apparent K_m for Na^+ binding of approximately 50mM and apparent K_m for P_i-.binding of the order of 0.1 mM, agree with the values obtained in studies with membrane vesicles and with cell culture models. The pH-dependency represents the hallmark of the renal proximal tubular brush border membrane Na^+/P_i-cotransport, whereby decreased transport

Correspondence to H. Murer

rates occur at high proton concentrations (Amstutz et al., 1985; Hoffman et al., 1976).

Recently a Na^+/P_i cotransporter which satisfies the criteria for membership of the type II family has also been cloned from winter flounder (*Pseudopleuronectes americanus*) (Werner et al., 1994). In contrast to the mammalian kidney, P_i handling in the fish kidney involves both tubular reabsorption and secretion (Renfro & Gupta, 1990). This special feature could reflect the situation in mammalian kidneys under pathological or extreme conditions of P_i homeostatic imbalance (Berndt & Knox, 1992).

The flounder type II Na^+/P_i cotransporter (hereafter designated as NaPi-5) was shown to share most of the functional and structural features with other members of mammalian type II Na^+/P_i cotransporters. At the primary structural level, 80% sequence identity is found between rat type II isoform (NaPi-2) and NaPi-5 within the putative membrane spanning segments in contrast to the hydrophilic parts which reveal little homology (Werner et al., 1994). This cotransporter shows distinct differences from its mammalian counterparts with regard to tissue distribution and intracellular sorting. NaPi-5 is expressed in kidney as well as in intestine and in kidney it is localized basolaterally in the secreting part of the tubule whereas the intestinal protein is found in the apical membrane (Kohl et al., 1996).

So far the functional characterization of NaPi-5 has been limited to flux measurements using the *Xenopus laevis* oocyte expression system. To characterize the transport kinetics and allow a detailed comparison with other members of the type II family, a more sensitive assay was considered necessary. We therefore re-evaluated the functional characteristics of NaPi-5 electrophysiologically, including both steady-state and presteady-state analysis. The magnitude of the P_i-induced currents for expressed NaPi-5 (up to 1000 nA at −100 mV) was a prerequisite for attempting the latter analysis: in expression studies of the human, murine and rat type II Na^+/P_i-cotransporters (Busch et al., 1994, 1995; Hartmann et al., 1995), steady-state currents an order of magnitude smaller have been observed. The concomitantly smaller presteady-state relaxations become difficult to resolve with the two-electrode voltage clamp technique used under all substrate and membrane potential conditions (Forster et al., 1996). Kinetic analysis of presteady-state currents have been performed recently for other sodium coupled transporters (e.g., Wright et al., 1996). These studies have demonstrated that this technique is an important tool for characterizing transport rates for cotransporter families and can provide insights into the partial reactions of the transport cycle.

Materials and Methods

In vitro preparation of cRNA encoding NaPi-5 has been previously described (Werner et al., 1994) and the dissection of *Xenopus laevis* ovaries, collection and handling of the oocytes have been detailed elsewhere (e.g., Busch et al. 1992). Oocytes were injected with 10–14 ng (50 nl) cRNA/oocyte or 50 nl water.

Steady-state Measurements

Recordings were performed at room temperature 1–8 days after injection using a commercial two electrode voltage-clamp (Geneclamp 500, Axon Instruments, Foster City, CA). If not otherwise stated, the holding potential was −50 mV and the data were filtered at 10 Hz and recorded with MacLab hardware and compatible software for data acquisition and analysis (AD Instruments, Castle Hill, Australia). The external control solution (superfusate) contained (in mM): 96 NaCl, 2 KCl, 1.8 $CaCl_2$, 1 $MgCl_2$ and 5 N-hydroxyethylpiperazine-N′-2-ethanesulfonic acid (HEPES). Phosphate was added to this solution at the indicated concentrations. The final solutions were titrated to the pH indicated using HCl or NaOH. To study the Na^+ dependence of P_i-induced currents, NaCl was partially replaced by choline chloride. In those experiments KOH was used instead of NaOH for titration. The flow rate of the superfusion was 20 ml/min and a complete exchange of the bath solution was reached within about 10 sec. The steady-state currents (I_p) stated are the maximal values measured during a 30-sec substrate superfusion. Pooled data are shown as mean ± SEM (n) where n represents the number of cells. The size of I_p varied 2–5-fold, depending on the time of measurement after cRNA injection and on the batch of oocytes (from different animals). Therefore, we show experimental data obtained on the same day for each specific set of experiments, unless otherwise indicated. Pooled data were tested for significance using the paired student's t-test and only results with $P < 0.05$ were considered as significant. Dose-response data were fit to the modified Hill equation (*see below*), using a nonlinear regression analysis routine supplied with MacLab software.

Presteady-state Measurements

Electrophysiology was performed using a laboratory-built two electrode voltage clamp, optimized for fast voltage clamping of the oocyte membrane (true membrane potential 10–90% rise time, typically <0.5 msec) using electronic compensation for the bath series resistance. Oocytes were continuously superfused in a small chamber (approx. volume 200 μl) at 6 ml/min. Data were acquired using custom built AD/DAC hardware and DATAC software (Bertrand & Bader, 1987), sampled at 50 or 100 μsec/point and filtered at 5 or 3 kHz using an 8-pole Bessel filter (Frequency Devices, Haverhill MA, Model 902). Exponential curve fitting was performed using a Chebychev transform-based routine written C language (G. Malachowski, *personal communication*). Hill equation and Boltzmann fits (*see below*) were performed using the nonlinear regression analysis routines supplied with Inplot/Prism software (Graphpad, San Diego, CA). The control superfusate was the same as for the steady-state measurements but with equimolar substitution of barium for calcium to reduce contamination from Ca-activated Cl^- currents. For sodium replacement experiments, N-methyl-D-glucamine was substituted for sodium and titrated to pH 7.4 with HCl. All presteady-state experiments were performed at 18 ± 0.5°C.

Typical data recordings for each experiment are shown for one representative oocyte. Protocols were repeated for cells from the same batch and other batches to generate the pooled data as indicated.

Nonlinear Regression Analysis Fit Equations

Modified Hill Equation for Substrate Dose Response

Response with respect to a variable substrate S, were quantified as peak P_i-induced current (I_p) and the dose response fitted to a form of the Hill equation:

$$I_p = I_{p\max}\,[S]^n/([S]^n + (K_m^s)^n) \quad (1)$$

where $[S]$ is the substrate concentration; $I_{p\max}$ the extrapolated maximum current, K_m^s the concentration of substrate S which gives a half maximum response or apparent affinity constant and n the Hill coefficient.

Two State Eyring-Boltzmann Model for Transmembrane Charge Movements

For a two state system in which a charged entity having an apparent valency z can translocate between states 1 and 2 within the transmembrane field over an energy barrier, the rate constants for the respective transitions $1 \Rightarrow 2$ and $2 \Rightarrow 1$, according to Eyring-Boltzmann kinetics (e.g., Jack et al., 1983), are given by:

$$k_{12} = A_o \exp(-ze\delta V/kT) \text{ and } k_{21} = B_o \exp((1-\delta)zeV/kT)$$

where V is the transmembrane voltage, e the electronic charge, k Boltzmann's constant, T the absolute temperature, A_o, B_o are the rate constants for $V = 0$ and δ is an asymmetry factor ($0 \leqslant \delta \leqslant 1$) defining the electrical distance to the energy barrier for the transition from state 1. For a voltage jump to a potential V, the induced charge movement will give rise to a current relaxation with a time constant τ given by:

$$\tau = 1/(k_{12} + k_{21})$$

i.e.,

$$\tau = 1/(A_o \exp(-ze\delta V/kT) + B_o \exp(ze(1-\delta)V/kT)) \quad (2)$$

The steady-state charge distribution at any voltage V for N independent charged entities is given by:

$$Q = Q_{\max}/(1 + \exp(-ze(V - V_{0.5})/kT))$$

where $Q_{\max} = Nze$, the maximum charge which can be translocated and $V_{0.5}$ is the voltage at which the charge is distributed equally between states 1 and 2, corresponding to the condition $k_{12} = k_{21}$. For a finite holding potential, V_h,:

$$Q = Q_{\text{hyp}} + Q_{\max}/(1 + \exp(-ze(V - V_{0.5})/kT)) \quad (3)$$

where: Q_{hyp} the charge at the hyperpolarizing limit which depends on V_h. Equations 2 and 3 were used for the nonlinear regression fitting to relaxation data.

Simulation of Three-State Kinetic Model

Simulations were performed by solving differential equations describing the kinetics using the standard matrix method for solution of eigenvalues and eigenvectors. Routines were written in C and adapted from those given in Press et al. (1992).

Results

Steady-state Behavior of NaPi-5 with Varying Substrate Concentrations and Holding Potentials is Consistent with Type II Na^+/P_i Cotransport

Superfusion of *Xenopus* oocytes expressing NaPi-5 with P_i (1 mM) induced an inward current (I_p) of −276 ± 26 nA ($n = 4$) in the voltage-clamp mode at a holding potential, $V_h = -50$ mV and a depolarization from −43 ± 3 mV to −17 ± 3 mV ($n = 4$) under current clamp conditions (zero current applied). Thus, in NaPi-5 expressing oocytes, P_i induces an apparent net inward movement of positive charges as previously described for the mammalian type II Na^+/P_i cotransporters (Busch et al. 1994, 1995). In water-injected control oocytes no significant inward current or depolarization was observed (*data not shown*).

Figure 1*A* shows a typical family of P_i-induced currents with P_i varying over three decades for 96 mM Na^+ and $V_h = -50$ mV, which indicates clear evidence of saturation for $P_i > 0.3$ mM. The normalized dose-response behavior, pooled for 4 cells, is quantified in Fig. 1*B* at two Na^+ concentrations. For both 96 mM Na^+ and 50 mM Na^+ the peak P_i-induced current, I_p, normalized to the maximum current $I_{p\max}$, at 96 mM Na^+/1 mM P_i shows a sigmoidal form on a semi-logarithmic scale. These data were fit to the modified Hill equation (Eq. 1, Materials and Methods) to give an apparent K_m for P_i (K_m^{Pi}) of 0.043 mM at 96 mM Na^+ and 0.080 mM at 50 mM Na^+, with a Hill coefficient of approximately unity in both cases (*see* legend, Fig. 1*B*). The observed increase in K_m^{Pi} with reduced Na^+ is consistent with the behavior reported for other type II Na^+/P_i cotransporters which have been characterized electrophysiologically (Busch et al., 1994, 1995). Moreover, the maximum P_i-induced current ($I_{p\max}$) was reduced by approx. 25% when superfusing with lower Na^+. Voltage dependence of I_p is a further characteristic of type II cotransporter behavior (Busch et al., 1994, 1995), which we also confirmed for NaP$_i$-5 as shown from the current-voltage relationship shown in Fig. 1*C*. With 96 mM Na^+/1 mM P_i, the steady-state current relative to that at −90 mV was linearly related to the holding potential, V_h, over the range −10 to −90 mV.

We next examined the voltage dependence of substrate/NaPi-5 interaction in the steady-state. The normalized dose-response behavior is quantified in Fig. 1*D* for three holding potentials ($V_h = -30, -50, -90$ mV) ($n = 5$). For all three V_h, the dose-response for I_p normalized to the maximum current, $I_{p\max}$ at −90 mV, shows a sigmoidal form on a semilogarithmic scale with saturation for $P_i > 0.3$ mM. Fitting these data to Eq. 1 gave $K_m^{Pi} \approx 0.03$ mM, which was independent of V_h and furthermore the Hill coefficient was approximately unity for each V_h (*see* legend Fig. 1*D*).

Figure 1*E* shows that with Na^+ as the variable substrate at a constant P_i of 1 mM, I_p depended on Na^+ with an apparent affinity constant (K_m^{Na}) of 46 ± 2 mM ($n = 5$) at a holding potential of −50 mV. In contrast to the voltage independent behavior when P_i was the variable substrate, the apparent Na^+ dose-response relation was voltage-dependent. Fitting these data to Eq. 1 showed that K_m^{Na} was shifted from 32 ± 1 mM at −90 mV

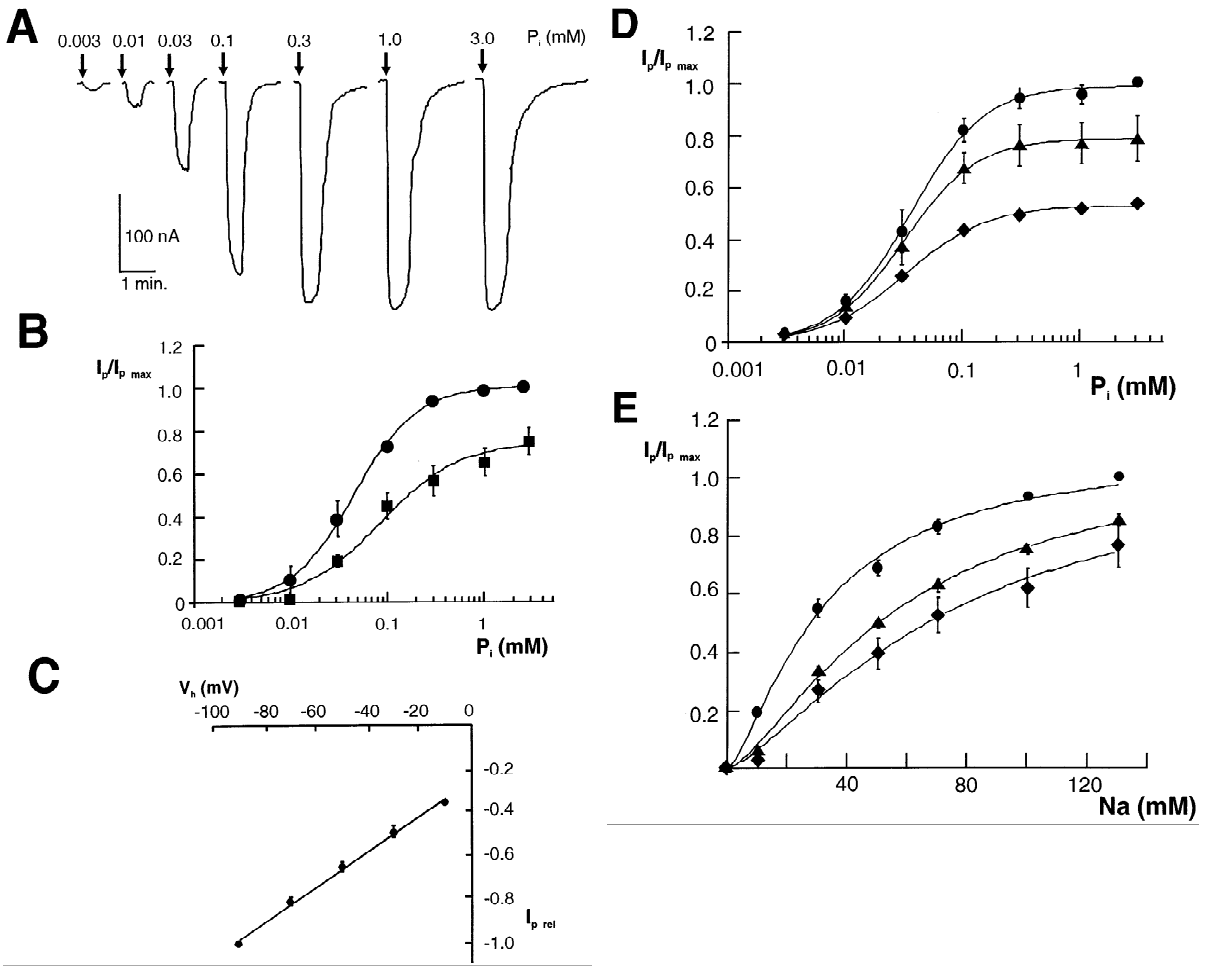

Fig. 1. Steady-state current characteristics of NaPi-5 expressing oocytes for varying substrate concentrations and holding potential. (*A*) Representative set of recordings from the same oocyte expressing NaPi-5 in response to different Pi concentrations indicated for 96 mM Na^+ and voltage clamped to a holding potential, $V_h = -50$ mV. P_i was applied at the time indicated by the arrows for 30 sec. After each application, the cell was perfused again with the control solution (*see* Materials and Methods) until the baseline was stable. (*B*) Steady-state dose response for P_i as the variable substrate at $V_h = -50$ mV with 96 mM Na^+ (●) and 50 mM Na^+ (■). Data points were derived from sets of responses as in *A*, normalized to the maximum I_p at 96 mM Na^+/1 mM P_i, and pooled from 5 oocytes. Continuous lines are nonlinear regression fits of the modified Hill equation to the normalized data. (Eq. 1, Materials and Methods). The K_m^{Pi} values (in mM) were: (96 mM) 0.043 ± 0.004; (50 mM) 0.080 ± 0.025. The differences for K_m^{Pi} are significantly different at the $P < 0.05$ level ($n = 5$). The Hill coefficients were: (96 mM) 1.0 ± 0.03; (50 mM) 0.8 ± 0.1 and are not significantly different at the $P < 0.05$ level ($n = 5$). (*C*) Steady-state current voltage relationship for NaPi = 5 at 96 mM Na^+/1 mM P_i showing the effect of holding potential V_h on P_i-induced current. Ordinate scale ($I_{p\,rel}$) is the steady-state current relative to the response at $V_h = -90$ mV. Continuous line is a best fit linear regression. (*D*) Dose-response relation for P_i as the variable substrate at $V_h = -90$ mV (●), −50 mV (▲) and −30 mV (♦). Data points were derived from sets of responses as in *A* and pooled from 5 oocytes. All data were normalized to the maximal current at −90 mV and 96 mM Na^+/1 mM P_i. Continuous lines are nonlinear regression fit of the modified Hill equation to the normalized data (Eq. 1, Materials and Methods). The K_m^{Pi} values (in mM) were: (−90 mV) 0.035 ± 0.001; (−50 mV) 0.031 ± 0.001; (−30 mV) 0.032 ± 0.001. The Hill coefficients were: (−90 mV) 0.9 ± 0.1; (−50 mV) 1.1 ± 0.1; and (−30 mV) 0.8 ± 0.1. The differences for K_m^{Pi} and Hill coefficients at the each holding potential are not significant at the $P < 0.05$ level ($n = 5$). (*E*) Dose-response relation for Na^+ as the variable substrate at $V_h = -90$ mV (●), −50 mV (▲) and −30 mV (♦) holding potential and $P_i = 1$ mM. All data were normalized to the maximal current at −90 mV at 96 mM Na^+. The continuous lines are nonlinear regression fits of the modified Hill equation to normalized data. The K_m^{Na} values (in mM) were: (−90 mV) 32 ± 1; (−50 mV) 46 ± 2; (−30 mV) 77 ± 2. The Hill coefficients for Na^+ were: (−90 mV) 1.5 ± 0.1; (−50 mV) 1.7 ± 0.1 and (−30 mV) 1.5 ± 0.1. The differences for K_m^{Na} at the different holding potentials are significant at the $P < 0.05$ level ($n = 5$).

to 77 ± 3 mM at −30 mV (Fig. 1*E*, $n = 5$). Moreover, the Hill coefficient for the apparent Na^+ affinity was between 1 and 2 (*see* legend, Fig. 1*E*) suggesting a cooperative reaction in which more than one Na^+ ion binds per transport cycle.

NaP_i Steady-state Transport is pH Dependent

As phosphate transport in mammalian as well as in flounder renal cells is influenced by pH (Amstutz et al., 1985; Gupta et al., 1991) we next examined the effect of

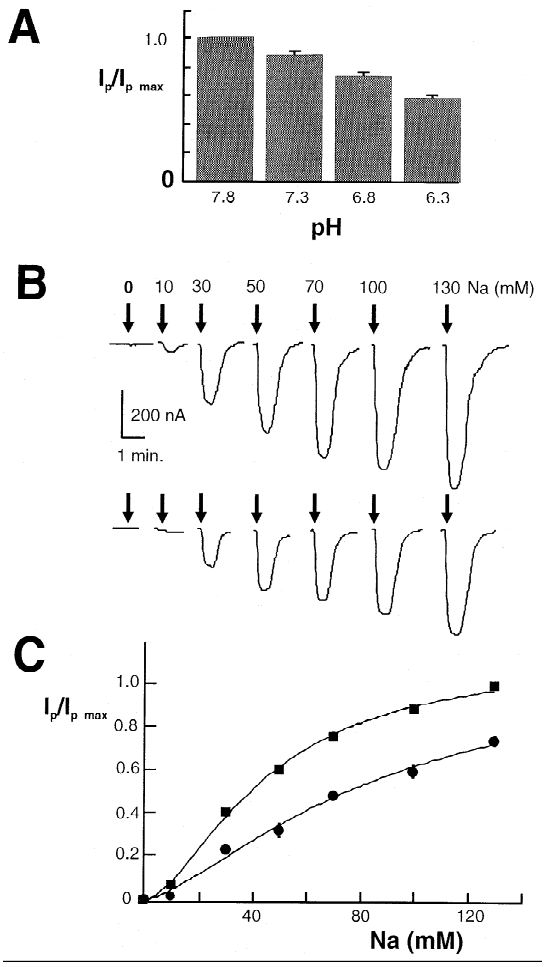

Fig. 2. Dependency of NaPi-5 expressing oocytes on superfusate pH. (*A*) The P_i-induced steady-state current decreases with pH. Pooled results from 5 oocytes showing the effect on I_p of decreasing pH from 7.8 to 6.3 (96 mM Na^+/1 mM P_i). All data were normalized to the maximum current at pH 7.8. All differences are significant at $P < 0.05$ ($n = 5$). (*B*) Recordings from the same oocyte showing the effect of pH on the Na^+-dependence of I_p, at 1 mM P_i and $V_h = -50$ mV. Arrows indicate the beginning of 30 sec. superfusion with P_i at different Na^+ concentrations indicated for pH 7.5 (upper traces) and pH 6.5 (lower traces). (*C*) Dose-response relation for Na^+ at pH 7.5 (■) and pH 6.5 (●). All data were normalized to the maximum current at 130 mM Na^+ at pH 7.5 (I_{pmax}). The curves were obtained by fitting the data to Eq. 1. In this case, the maximum extrapolated current was 1.1 and the K_m^{Na} values (in mM) were: (pH 7.5) 46 ± 1; (pH 6.5) 89 ± 3. The corresponding Hill coefficients were: (pH 7.5) 1.7 and (pH 6.5) 1.8 ($n = 5$).

pH on I_p under conditions of constant, saturating P_i (=1 mM). As shown in Fig. 2*A*, raising pH from 6.3 to 7.8 resulted in a significant increase of I_p by about 50% ($n = 5$). For the mammalian type II Na^+/P_i cotransporter from rat it has been shown that the pH-dependency of I_p is consistent with protons interacting with Na^+ ions at the Na^+ binding site on the Na^+/P_i cotransporter (Amstutz et al., 1985, Busch et al., 1994) to result in a decreased transport of P_i. For the typical set of recordings from the same oocyte shown in Fig. 2*B*, in addition to the smaller P_i-induced currents, a shift in pH from 7.5 to 6.5 gives a clearly observable change in the Na^+ binding. This behavior is quantified in Fig. 2*C*, where fitting the dose-response to Eq. 1 indicated a significant shift in K_m^{Na} from 46 ± 1 to 89 ± 3 mM ($n = 5$). For both pH conditions, the Hill coefficient for apparent Na^+ affinity was close to 2 (*see legend*, Fig. 2*C*).

Voltage Steps Induce Presteady-state Charge Movements in NaPi-5 Expressing Oocytes

The level of expression for NaPi-5 indicated by the magnitude of steady-state currents allowed us to investigate in NaPi-5-expressing oocytes also displayed presteady-state relaxations as reported for other electrogenic Na^+-coupled cotransporters (e.g., Hazama et al., 1997; Wadiche et al., 1995). When voltage steps from holding potential of −100 mV were applied to oocytes expressing NaPi-5, a current relaxation was observed which was superimposed on the normal capacitive charging transient (Fig. 3*A*, left panel). This relaxation was absent if the cell was superfused with saturating P_i (1 mM) (Fig. 3*A*, center panel) and was suppressed in the absence of external Na^+ (Fig. 3*A*, right panel). This latter finding indicates that the P_i-suppressed relaxations were induced by the presence of Na^+ in the external medium. Furthermore, relaxations were not observed in non-injected oocytes from the same batch under the same superfusion conditions (Fig. 3*B*).

To characterize these relaxations further, we fitted them to multiple exponentials after each voltage step. For both the ON transition (step from holding potential) and OFF transition (step back to holding potential), good fits were obtained with two exponentials (Fig. 3*C*). The voltage dependence of the fitted time constants is shown in Fig. 3*D*, which confirms that the two components were separated by at least a factor of 5 except at extreme hyperpolarizing potentials. The fast component (τ_1, typically 400 μsec), which showed no detectable voltage dependence, was the same for both ON and OFF transitions and arises from the endogenous capacitive charging transient of the oocyte. The slower component (τ_2) has a ''bell''-shaped voltage dependence for the ON transition but no significant voltage dependence for the OFF transition. Furthermore, the mean $\tau_{2\text{-OFF}}$ at −100 mV for the eleven OFF transitions from −140 to +80 mV (2.60 ± 0.10 msec) lies between $\tau_{2\text{-ON}}$ at −80 mV and $\tau_{2\text{-ON}}$ at −120 mV. The apparent intersection of the two sets of data suggests that the same kinetic component has been detected from the fits to the ON and OFF relaxations. Such behavior would also be consistent with that of a transmembrane charge movement, the kinetics of which depend on the transition target potential.

As shown in Fig. 3*E*, the ON charge transfer (Q_{ON}) and OFF charge transfer (Q_{OFF}) are very similar over the

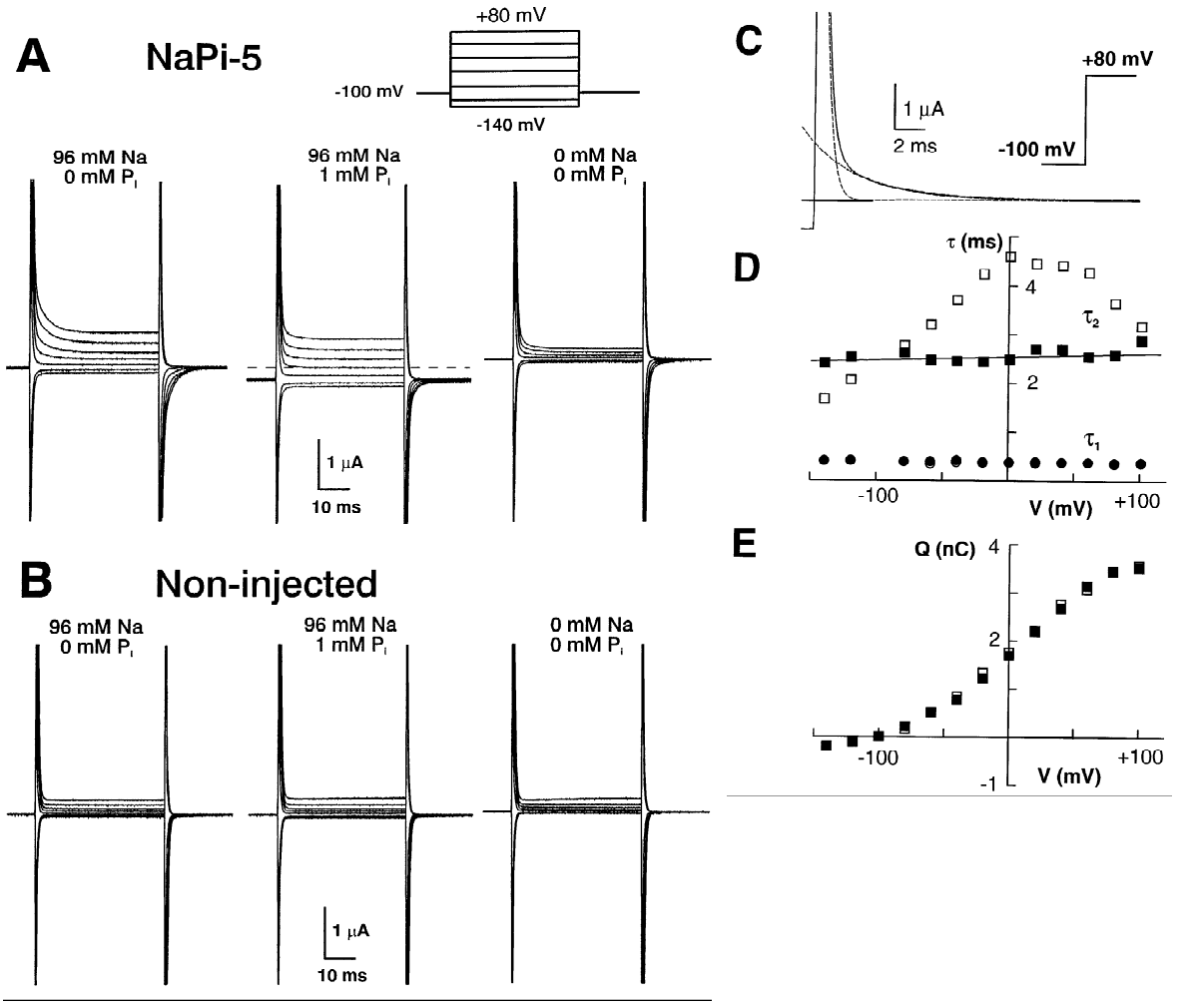

Fig. 3. Presteady-state relaxations induced by voltage steps applied to an oocyte expressing NaPi-5. (*A*) Presteady-state relaxations recorded from the same oocyte for the superfusion conditions indicated in response to voltage steps from a holding potential of −100 mV to −140, −120, −80, −40, 0, 40, 80 mV for 40 msec (*see* inset). Each current trace is the average of 8 sweeps, sampling 50 μs/point, 5 kHz filtering. Complete transient currents have been cutoff to aid visualization. The dashed line indicates the steady-state response at −100 mV for 96 mM Na^+/0 mM P_i. The downward shift of the baseline at −100 mV in the presence of P_i (center panel) compared to the records in the absence of P_i (left panel) is due to the P_i-induced steady-state current, $I_p \approx -210$ nA. The baseline shift for 0 mM Na^+/0 mM P_i (right panel) results from a change in the oocyte leakage current in the absence of Na^+. Superfusion with 0 mM Na^+/1 mM P_i did not induce a measurable difference in the records compared with those without P_i (*data not shown*). (*B*) The response of a non-injected oocyte from the same batch as in *A* to the same voltage step and superfusion conditions shows no P_i-induced current (center panel) and no relaxations in addition to the intrinsic membrane charging component (left and center panels). The outward current seen for steps to +80 mV can be attributed to the activation of endogenous Cl^- channels. (*C*) Expanded view of the step transition from −100 to +80 mV in the presence of 96 mM Na^+/0 mM P_i from the data in *A*. Dashed lines show the two exponential components found by applying a bi-exponential fit to the data (τ_1 = 360 μs; τ_2 = 3.7 msec). The original bi-exponential fit is indistinguishable from the raw data. (*D*) Voltage-dependence of fitted time constants for bi-exponential fit to presteady-state relaxations for same cell as in *A* with 96 mM Na^+/0 mM P_i. Open symbols are for the ON transitions (step from −100 mV holding potential), filled symbols are for the OFF transitions (return step to −100 mV). Fast component (τ_1): ●,○; slow component (τ_2): ■,□. For τ_1 the ON and OFF τs are indistinguishable. Continuous line is a linear regression applied to τ_{2OFF} for steps from −140 to +80 mV, giving a slope not significantly different from zero. (*E*) Voltage-dependence of equivalent charge transfer for slower component in *D*. Open symbols are for the ON transition (step from −100 mV holding potential) and filled symbols are for the OFF (return step to −100 mV). Charge was found by backward extrapolation of the fitted component to 1 msec after the step transition.

voltage range used and the direction of charge movement reverses at the holding potential. This finding indicates the charge movements are capacitive in nature. Furthermore, the *Q-V* data show a tendency to saturate at both extremes of potential. Taken together with the τ-*V* data, these *Q-V* data are also consistent with the slower relaxation component being a nonlinear transmembrane charge movement.

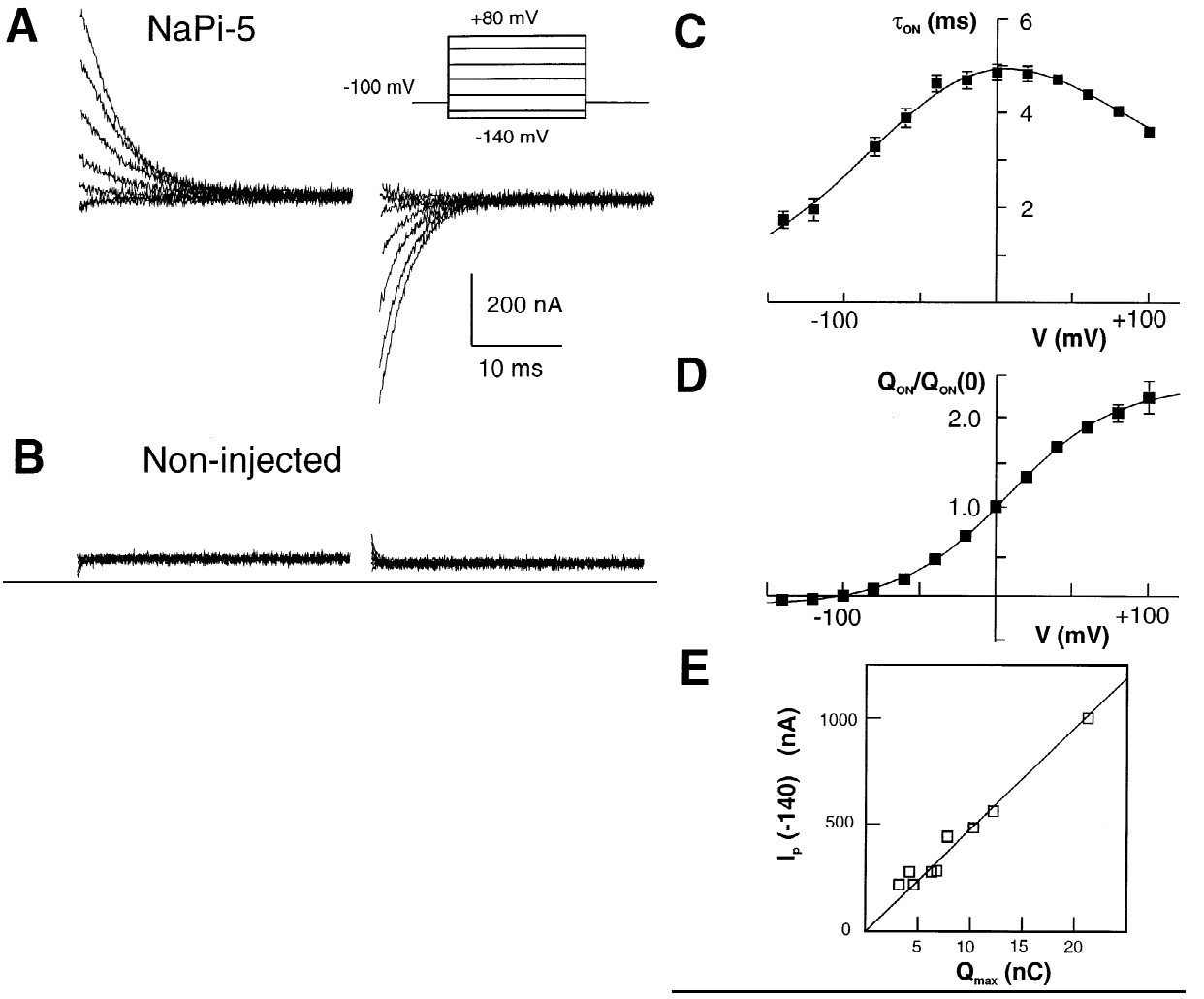

Fig. 4. Characterization of P_i-suppressed presteady-state relaxation kinetics. (*A*) Suppression of presteady-state relaxations by 1 mM P_i in the presence of 96 mM Na^+, for the same cells as in Fig. 3 *A* and *B* and the same voltage steps. Each record is the difference between the record without P_i and with a saturating (1 mM) P_i and is a measure of the charge suppressed by P_i. The steady-state offsets have been subtracted and records blanked for the first 1.5 msec after the voltage transition because during this interval the time course of apparent charge movement is influenced by the voltage clamp and oocyte membrane charging. (*B*) Response from non-injected oocyte to same protocol as in *A*. (*C*) Time constant for relaxation after ON transition, (τ_{ON}) found from single exponential fit to records in *A*, plotted as a function of voltage, (mean ± SEM ($n = 9$)). Continuous line is nonlinear regression fit to Eq. 2 (*see* Materials and Methods). For the fit shown, $A_o = 60 \pm 10$ sec^{-1}, $B_o = 140 \pm 10$ sec^{-1}, $\delta = 0.67 \pm 0.04$; $z = 0.55 \pm 0.02$. (*D*) Normalized Q_{ON}-*V* relation obtained by integrating the P_i-suppressed relaxations as in *A*, pooled and normalized to the value of Q_{ON} at 0 mV, for the same 9 cells as in *C*. Continuous line is a nonlinear regression fit to Eq. 3 (*see* Materials and Methods). For fit shown: $V_{0.5} = +8 \pm 1$ mV and $z = 0.71 \pm 0.02$. (*E*) Correlation between the magnitude of the P_i-induced steady-state current at −140 mV ($I_p(-140)$) and total charge movement Q_{max}) predicted from Boltzmann fit to Q_{ON}-*V* data for 10 oocytes from different batches. Straight line is a linear regression fit, forced through the origin giving a slope of 50 sec^{-1}.

Characteristics of the P_i-suppressed Relaxations

To characterize further the P_i-suppressed relaxations we subtracted the records with 1 mM P_i from those with 0 mM P_i, both in the presence of 96 mM Na^+. In addition to the steady-state P_i-induced current, this procedure gives the P_i-suppressed relaxations directly and eliminates any oocyte endogenous component of the capacitive transient which might otherwise influence the accuracy of the curve fitting procedure. Furthermore, it suppresses contamination from endogenous Cl^- currents which sometimes appeared at high depolarizing potentials, depending on the oocyte batch. Figure 4*A* shows a typical family of P_i-suppressed relaxations for the ON and OFF transitions with the steady-state currents subtracted. No significant relaxations were observed for the non-injected oocyte under the same conditions (Fig. 4*B*).

We found that fitting the relaxation component to a

single exponential could describe the relaxation time course satisfactorily and by integrating the difference records, we obtained an estimate of the apparent charge movement suppressed by saturating P_i. Figure 4*C* shows that the pooled, fitted time constant ($n = 9$) for the ON-relaxation (τ_{ON}) has a similar bell-shaped voltage dependence as was obtained by fitting the total, unsubtracted relaxation (Fig. 3*D*). Furthermore, the *Q-V* data for the same cells, normalized to Q_{ON} at 0 mV to take account of different levels of expression, show saturation (Fig. 4*D*) at both extremes of potential. The τ_{ON}-*V* and Q_{ON}-*V* data of Fig. 4*C* and *D* respectively could be well fit to the corresponding equations for a simple two state model, based on Eyring-Boltzmann transition rate theory (Eqs. 2 and 3, Materials and Methods). For the Q_{ON}-*V* data, the Boltzmann fit gave a midpoint voltage = +8 mV and an apparent valency, $z = 0.7$. The fit to the τ_{ON}-*V* data gave $z = 0.6$ and an asymmetrical barrier located a fractional electrical distance $\delta = 0.6$ from the external medium. We noted that forcing the fit to have a symmetrical barrier ($\delta = 0.5$) gave a significantly poorer fit to the data.

Finally, as shown in Fig. 4*E*, if the maximum steady-state current at V = −140 mV ($I_p(-140)$) for 96 mM Na^+/1 mM P_i, derived from the plateau of the presteady state records, is plotted against Q_{max} predicted from the Boltzmann fit for different oocytes from different batches, a linear correlation is found with a slope of 50 sec^{-1}. This finding strongly suggests that the P_i-suppressed charge movement is related to functional NaPi-5 cotransporters.

Presteady-state Behavior with Varying Substrate Concentrations

Since both substrates transported by NaPi-5 bear electrical charges, these relaxations could arise from the binding/release of one or other of the substrates with NaP_i-5 and/or charge movements associated with the unloaded or partially loaded carrier. To identify the source of these relaxations more precisely, we performed experiments under conditions of varying substrate concentrations.

Varying P_i

Figure 5*A*, shows typical recordings for voltage steps from −100 mV to the voltage indicated for four P_i concentrations, which were chosen to cover the sloping region of the steady-state dose-response characteristic (*see* Fig. 1*B*). In each case Na^+ was fixed at 96 mM. To characterize the effect of changing P_i, we subtracted the record for 0 mM P_i from the corresponding record at the test P_i, at each potential. The difference record shows the P_i-induced steady-state current at −100 mV and the test potential, with the P_i-suppressed relaxations superimposed at the ON and OFF transitions. The initial amplitude of these relaxations increases with P_i but qualitatively there appears to be little change in the time course of the relaxation. The equivalent ON-charge of the relaxation alone, after subtracting the steady-state components and plotted as a function of P_i, (Fig. 5*B*) on a semilogarithmic scale shows a sigmoidal relation, similar to that obtained for the steady-state current (Fig. 1*B*). If these data are fit to the modified Hill equation (*see* Materials and Methods), the midpoint P_i concentration is only weakly dependent on potential (varying from 0.03 mM at 0 mV to 0.05 mM at −80 mV) and is close to K_m^{Pi} determined from the steady-state analysis (0.03 mM). As shown in Fig. 5*C*, over the voltage range −140 to +40 mV, the single exponential component found from fitting the relaxations, τ_{ON}, is independent of P_i. Moreover, Boltzmann fits to the Q_{ON}-*V* data shown in Fig. 5*D*, gave a similar *z* and $V_{0.5}$ which shifts only 20 mV for a 10-fold change in P_i (*see* legend, Fig. 5*D*). These findings suggest that the voltage dependence of the P_i-suppressed relaxations is little influenced by the P_i binding reaction. Together with the steady-state behavior of NaPi-5, they provide further support for a voltage independent P_i/NaPi-5 interaction.

(ii) Varying Na^+

To investigate the effect of Na^+ on NaPi-5 relaxation kinetics, we repeated the voltage step protocols with different Na^+ concentrations and 0 mM P_i. The range of Na^+ we used was limited to concentrations <100 mM because we were unable to obtain stable recordings for oocytes exposed to a hyperosmolar superfusate for long periods. Nevertheless, based on our finding that the steady-state voltage dependence for P_i-induced transport is Na^+-dependent (Fig. 1*C*), superfusing at concentrations <100 mM Na^+ was expected to result in a significant change in the relaxation kinetics in the presteady-state. Typical recordings are shown in Fig. 6*A*, where the ON and OFF relaxations are shown for voltage steps from a holding potential of −100 mV to five test potentials. These data indicate that for hyperpolarizing steps, the amount of charge transferred appears to be larger for 25 mM Na^+ than 96 mM Na^+. Furthermore, for depolarizing steps, the relaxation kinetics appear faster at 25 mM Na^+. These observations were quantified by exponential curve fitting to give the τ-*V* and Q-V relations for the ON transitions, shown in Fig. 6*B* and *C*, respectively. Reducing Na^+ resulted in significant changes in the relaxation voltage dependence: the peak of the τ-*V* data shifted to more hyperpolarizing potentials, the maximum $\tau_{(ON)}$ decreased and the $\tau_{(ON)}$-*V* data became skewed such that relaxation rates at potentials to the right of the peak were faster, whereas those to the left of the peak

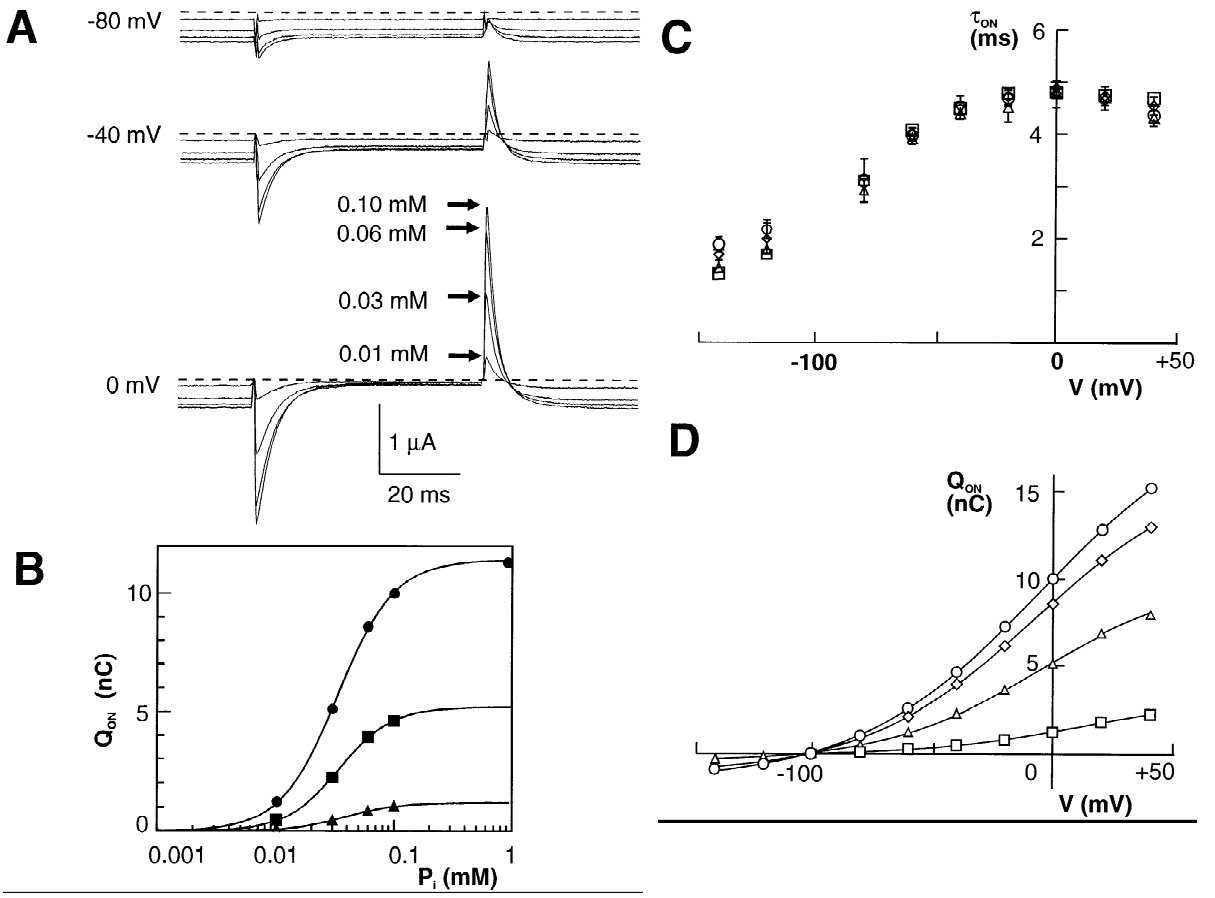

Fig. 5. Characteristics of presteady-state kinetics with varying P_i concentration. (*A*) Typical recordings of currents from the same oocyte for voltage jumps to the indicated potential for 60 msec from a holding potential of −100 mV for four concentrations of P_i indicated. Each record is the difference between the record in the presence of P_i and the corresponding record with 0 mM P_i. The dashed line indicates the zero current level in each case. (*B*) Dose response of the P_i-suppressed charge obtained by integrating the relaxations alone plotted as a function of P_i for the same cell and same test potentials (● = 0 mV; ■ = −40 mV; ▲ = −80 mV). Continuous lines are nonlinear regression fits to data points using Eq. 1 giving, for $V = 0$ mV, $n = 1.68$, $K_m^{Pi} = 0.03$ mM; $V = -40$ mV, $n = 1.17$, $K_m^{Pi} = 0.04$ mM and V = −80 mV, n = 1.6, $K_m^{Pi} = 0.05$ mM. (*C*) τ_{ON}-*V* data obtained from single exponential fits to P_i-suppressed relaxations, pooled from 4 representative oocytes for P_i (mM): □ = 0.01; Δ = 0.03; ◇ = 0.06; ○ = 0.1. (*D*) Q_{ON}-*V* for a single oocyte for the same P_i as above. Continuous lines are nonlinear regression fits of Eq. 3 to the data, giving: (□: 0.01 mM P_i) $z = 0.8$, $V_{0.5} = +14$ mV; $Q_{max} = 3.4$ nC; (△: 0.03 mM P_i) $z = 0.8$, $V_{0.5} = -5$ mV, $Q_{max} = 10.5$ nC; (◇: 0.06 mM P_i), $z = 0.7$, $V_{0.5} = -7$ mV, $Q_{max} = 18$ nC; (○: 0.1 mM P_i) $z = 0.7$, $V_{0.5} = -5$mV, $Q_{max} = 22$ nC.

were slower. Changes in the Q_{ON}-*V* relations were also observed (Fig. 6*C*): fitting to the Boltzmann equation (Eq. 3, Materials and Methods) showed a significant negative shift in the midpoint potential as Na^+ was reduced and the Q_{ON}-*V* curves appeared to flatten. This effect is more clearly apparent from the normalized Q_{ON}-*V* data (*see* inset and legend, Fig. 6*C*).

For 0 and 10 mM Na^+ we were also able to detect a relaxation superimposed on the capacitive charging component for large (>40 mV) jumps. However, over the voltage range possible with the two electrode voltage clamp, no charge saturation occurred, as shown in Fig. 6*C*, and meaningful fitting to the Boltzmann equation was not possible for 10 mM Na^+. Furthermore, for small voltage steps it was difficult to obtain reproducible separation by curve fitting due to the intrinsic noise on the data and the closeness of the time constant to the intrinsic oocyte capacitive transient.

The pooled fitting results are summarized in the Table. At each Na^+ concentration, the fits to the *Q*-*V* and τ-*V* data predict approximately the same apparent valency, which decreases with decreasing Na^+ from 0.6 at 96 mM to 0.3 at 25 mM. In contrast the maximum charge transfer, normalized to that at 96 mM Na^+, decreased by approximately 20% for a fourfold decrease in Na^+.

(iii) Varying pH

In a final set of experiments, we investigated the effect of pH on NaP_i-5 relaxations. This was prompted by the previously reported findings that protons can act as a substrate for a number of cotransporters and contribute to the presteady-state relaxations (e.g., Boorer et al., 1994,

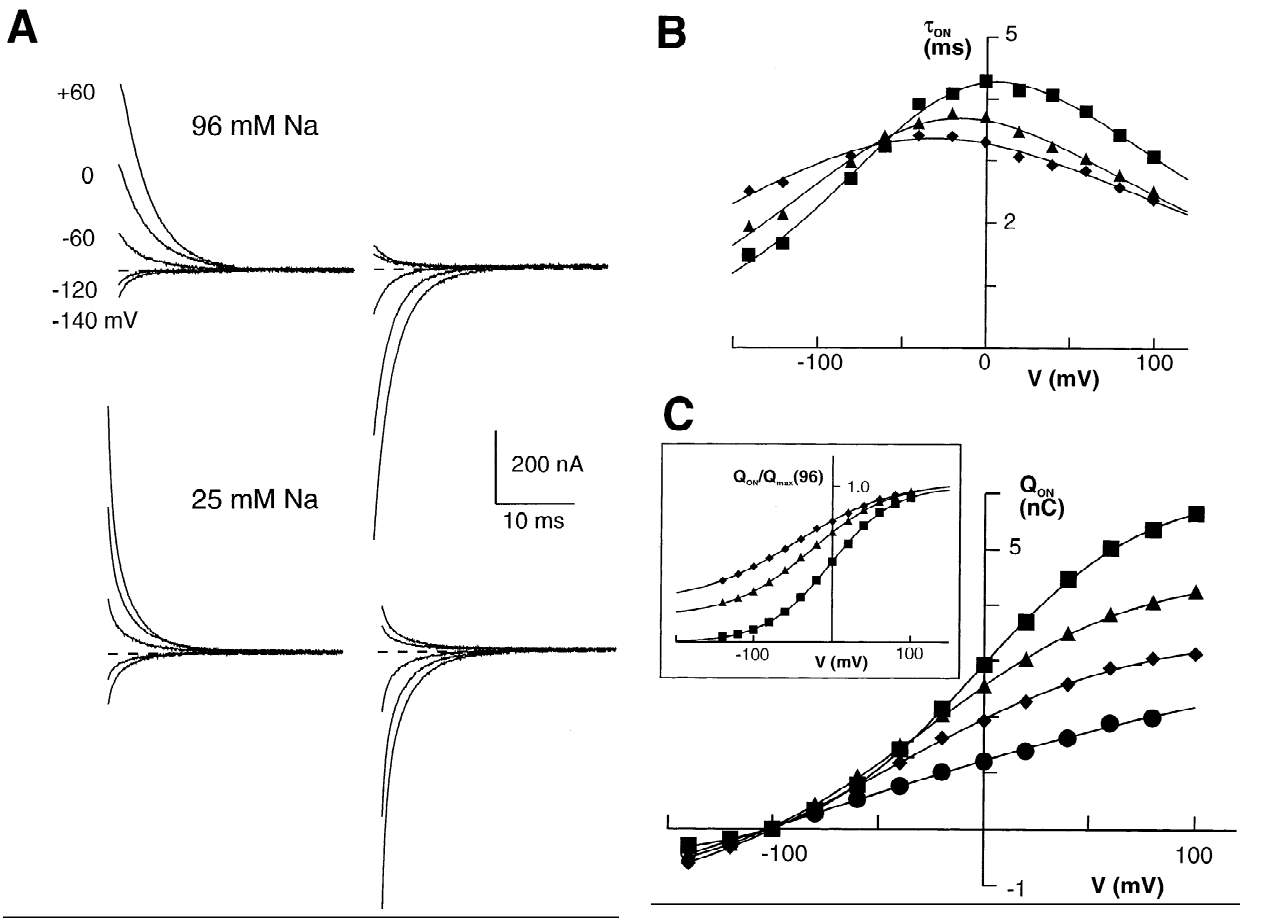

Fig. 6. Presteady-state kinetics with varying Na^+ concentration. (*A*) Typical presteady-state relaxations recorded from the same oocyte for Na^+ = 96 mM and 25 mM with voltage steps from −100 mV to −140, −120, −80, 0, +60 mV. For these records the first 1.5 msec during the capacitive charging of the oocyte have been suppressed. (*B*) τ_{ON}-*V* relation derived from single exponential fits to presteady-state relaxations from the cell in *A* for 96 mM Na^+ (■) and 50 mM Na^+ (▲) and 25 mM Na^+ (♦). Continuous lines are fits to Eq. 2 giving: (96 mM Na^+); A_o = 80 sec^{-1}, B_o = 150 sec^{-1}, z = 0.6, δ = 0.7; (50 mM Na^+); A_o = 70 sec^{-1}, B_o = 200 sec^{-1}, z = 0.5, δ = 0.7, (25 mM Na^+); A_o = 90 sec^{-1}, B_o = 220 sec^{-1}, z = 0.4, δ = 0.6. (*C*) Q_{ON}-*V* relation for relaxations at four concentrations of Na^+ (in mM): 96 (■); 50 (▲) and 25 (♦) and 10 (●)). The continuous lines are fits to Eq. 2, giving: (96 mM Na^+) z = 0.6, $V_{0.5}$ = −4 mV, Q_{max} = 6.68 nC; (50 mM Na^+) z = 0.5, $V_{0.5}$ = −26 mV, Q_{max} = 5.68 nC; (25 mM Na^+) z = 0.4, $V_{0.5}$ = −46 mV, Q_{max} = 5.12 nC. For 10 mM Na^+, the lack of saturation prevented obtaining a reliable fit to Eq. 3. Inset shows same data offest by Q_{hyp} obtained from each fit and normalized to Q_{max} for 96 mM Na^+. Boltzmann fits and data points have been superimposed at the depolarizing limit to show the shift in $V_{0.5}$.

1996) and our finding of pH dependence of steady-state P_i-induced currents for NaPi-5 (Fig. 2).

Figure 7*A* shows typical presteady state recordings for voltage steps from −100 to −140, −60, 0 and +60 mV for superfusion with 96 mM Na^+ at pH 7.4 and pH 6.2. These records show that relaxations are suppressed by the increase in H^+ concentration (from 0.04 μM to 0.63 μM). Quantification of these relaxations by bi-exponential curve fitting gave the τ_{on}-*V* data for the slower relaxation component and corresponding Q_{on}-*V* data shown Figure 7*B* and *C* respectively. For pH ranging from 7.4 to 6.2, the τ_{ON}-*V* data agree well, particularly for $V > 0$ mV, where reliable separation of the two exponential components was possible for this particular cell. The corresponding Q_{ON}-*V* data show that Q_{max} (*see* legend, Fig. 7), predicted from the single Boltzmann fit, is concomitantly reduced with increased external H^+. Relative to the steady state response at pH 7.4, I_p was reduced to 63 ± 6% (n = 6) at pH 6.8 and to 28 ± 3% (n = 6) at pH 6.2 under the same recording conditions. When Na^+ was removed from the external medium, no P_i-induced steady-state current could be detected at 1 mM P_i for a change in pH from 7.4 to 6.2 (*data not shown*). Furthermore, as shown in Fig. 7*D*, there was no detectable change in the relaxation time course for a pH change from 7.4 to 6.2. These findings indicate that for NaPi-5, protons neither substitute for Na^+ as a substrate nor contribute directly to the voltage dependence of the presteady-state relaxations under normal physiological conditions.

Table. Fit of two state Eyring-Boltzmann model equations to pooled *Q- V* and τ-*V* data with varying Na^+ concentration

Na^+ (mM)	Fit to Q_{ON}-*V* data*			Fit to τ_{ON}-*V* data*			
	Q_{max}/Q_{96}	$V_{0.5}$ (mV)	*z*	A_o (sec^{-1})	B_o (sec^{-1})	*z*	δ
96	1.0	−2 ± 3	0.6 ± 0.1	70 ± 20	150 ± 30	0.6 ± 0.1	0.7 ± 0.1
50	0.8 ± 0.1	−24 ± 4	0.5 ± 0.1	60 ± 20	200 ± 20	0.5 ± 0.1	0.7 ± 0.1
25	0.8 ± 0.1	−60 ± 9	0.3 ± 0.1	93 ± 20	200 ± 20	0.4 ± 0.1	0.6 ± 0.1

* mean ± SEM ($n = 4$)

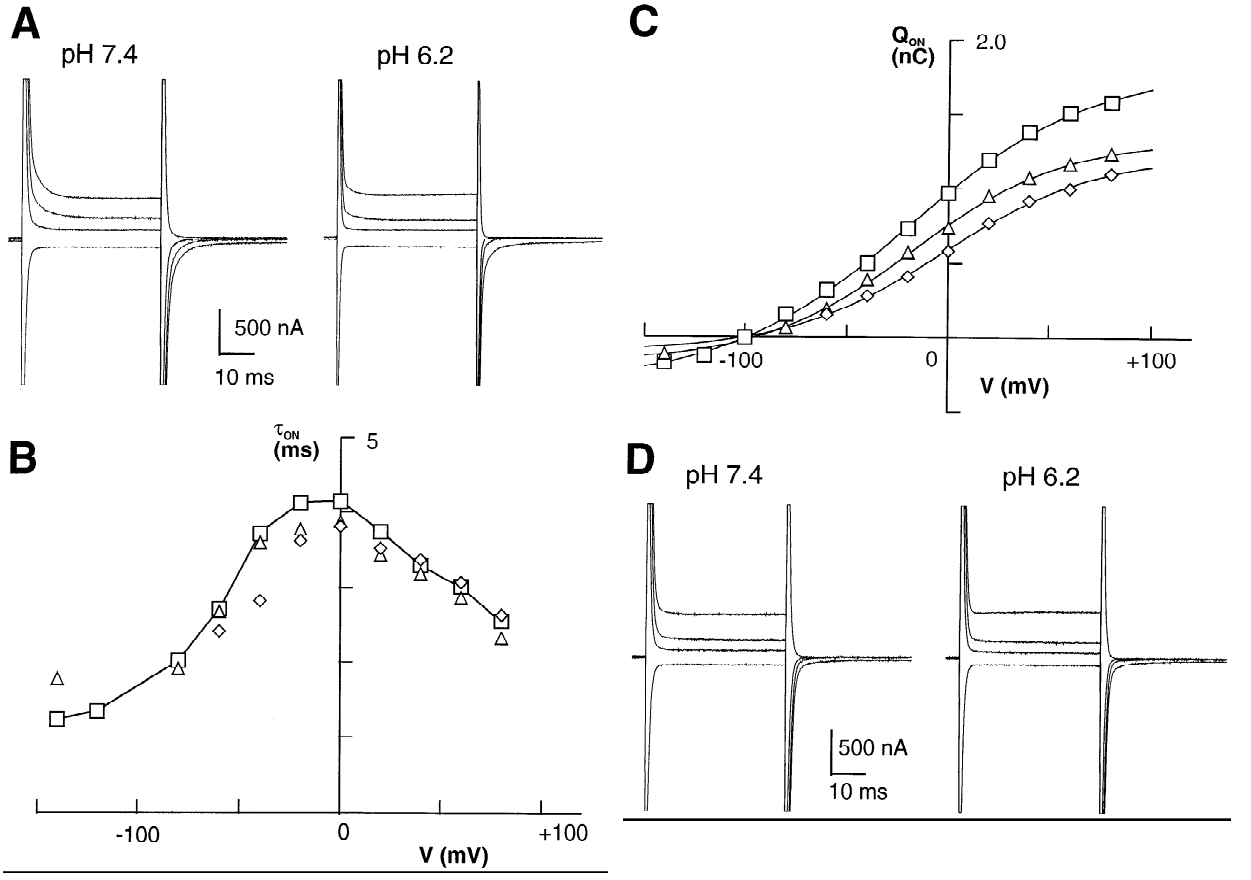

Fig. 7. The effect of changing external pH on NaPi-5 relaxations. (*A*) Presteady-state relaxations recorded in response to voltage jumps from a holding potential = −100 mV to −140, −60, 0, +60 mV, superfusing with 96 Na^+/0 mM P_i at the two pHs indicated. Records were made from the same oocyte with 8 averages, filtered at 5 kHz. (*B*) The τ_{ON}-*V* data for the slower time constant derived from exponential curve fitting relaxations from a representative oocyte for superfusion in 96 mM Na^+/0 mM P_i with pH 7.4 (□), pH 6.8 (△) and pH 6.2 (◇). Points at pH 7.4 have been joined by lines for visualization. *(C)* The corresponding Q_{ON}-*V* data for pH 7.4 (□), pH 6.8 (△) and pH 6.2 (◇). Continuous lines are fits to Eq. 3 giving the following parameters: pH 7.4: $V_{0.5} = -19$ mV, $z = 0.6$, $Q_{max} = 2.1$ nC; pH 6.8: $V_{0.5} = -18$ mV, $z = 0.7$, $Q_{max} = 1.5$ nC; pH 6.2: $V_{0.5} = -3$ mV; $z = 0.7$; $Q_{max} = 1.3$ nC. (*D*) Presteady-state relaxations recorded in response to voltage jumps from a holding potential = −100 mV to −140, −60, 0, + 60 mV for superfusion with 0 Na^+/0 mM P_i at the two pHs indicated. Same cell and same recording conditions in *A*.

Discussion

Steady-state Properties of NaPi-5

As reported in earlier studies of mammalian type II renal Na^+/P_i cotransporters such as NaPi-2 (rat), NaPi-3 and NaPi-7 (mouse), the flounder Na^+/P_i cotransporter NaPi-5, displays qualitatively similar steady-state characteristics (Busch et al., 1994, 1995, Hartmann et al., 1996). In particular, NaPi-5 shows high-affinity Na^+-dependent P_i-induced currents with a K_m^{Pi} which agrees in magnitude with earlier uptake studies of NaPi-5 expressed in *Xeno-*

pus oocytes (Werner et al., 1996). Furthermore, our finding that I_p is an inwardly directed current and strictly Na^+-dependent indicates that it is mediated by a net inward positive charge transfer as shown for its mammalian analogs, with a stoichiometry for Na^+ and P_i (e.g., 3:1), whereby the negative charge of the phosphate anion is overcompensated by cotransported Na^+ ions.

External Na^+ changed the apparent affinity for P_i which supports a model of ordered interaction between substrates and cotransporter as opposed to random binding models (e.g., Stein, 1990). Concomitant with the increase in apparent K_m^{Pi} with reduced Na^+, the maximum P_i-induced current at saturating P_i ($I_{p\max}$), was also suppressed. This behavior would be expected for ordered binding models in which Na^+ is the second substrate to bind (Stein, 1990). The lack of clear saturation for the Na^+ dose-response prevented us drawing further conclusions about the binding order of external substrates based on the steady state measurements alone. The Hill coefficient for apparent Na^+ binding never exceeded 2 in the present study, in further contrast to mammalian Na^+/P_i cotransporters, where a typical Hill coefficient of 3 was obtained for apparent Na^+ binding (Busch et al., 1994; Hartmann et al., 1995). Assuming a stoichiometry of at least 3:1 for NaPi-5, reduced cooperativity might result from independent Na^+ binding to more than one binding site. Moreover, the presence of an uncoupled Na^+ leak as described for the Na^+/glucose transporter (Umbach et al., 1990) may also influence the apparent cooperativity of Na^+ binding. The lack of a suitable high affinity blocker for Na^+/P_i cotransporters, such as phlorizin in the case of SGLT-1, precludes the straightforward electrophysiological measurement of uncoupled leak. At present we are unable to reach more definitive conclusions as to the stoichiometry of Na^+ binding to NaPi-5. More insight would be expected from studies involving labeled substrate uptake and electrophysiological measurements performed on the same cell (e.g., Klamo et al., 1996).

Membrane potential affected the apparent affinity for Na^+ at saturating P_i, but significantly did not affect the apparent K_m^{Pi} at 96 mM Na^+. Similar behavior has also been reported in studies on the human type II Na^+/P_i cotransporter isoform (NaPi-3) (Busch et al., 1995). As we observe a voltage dependency for the apparent K_m^{Na}, we would also expect this to be reflected in the apparent K_m^{Pi} since both K_m^{Pi} and $I_{p\max}$ are affected by Na^+. Our inability to detect such a voltage dependence in the apparent binding of P_i may result from a masking of the true P_i binding voltage dependence by that of Na^+ which occurs under nonsaturating Na^+ conditions present here. It should be noted in this context that the apparent affinity constant for each substrate is a complex function of the true affinity constant for that substrate and rate constants of other partial reactions in the transport cycle (e.g., Restrepo & Kimmich, 1985). Therefore the apparent affinity constants do not necessarily reflect the voltage dependence of binding for that substrate alone.

Steady-state transport rate was also pH-dependent, in agreement with previous findings from P_i uptake studies (Werner et al., 1994) and this behavior was consistent with the notion that protons compete for occupancy of the Na^+ binding site (Amstutz et al., 1985). The effect of pH on I_p was qualitatively consistent in both the steady-state and presteady-state measurements, however the faster superfusion and solution exchange possible with the presteady-state recording setup may account for the greater sensitivity to pH observed. Changes in pH influenced the steady-state kinetics of NaPi-5 less than its mammalian analogs (Busch et al., 1994, 1995; Hartmann et al., 1995). For example, decreasing the pH from 7.5 to 6.5 increased the apparent K_m^{Na} about threefold for the rat NaPi-2 (Busch et al., 1994), whereas the apparent K_m^{Na} for NaPi-5 increased only about twofold for the same change in pH. Significantly, the Hill coefficient for apparent Na^+ binding was essentially pH independent indicating that H^+ ions affect the affinity but not the cooperativity of this reaction.

Presteady-state Relaxations and NaPi-5 Turnover

The characterization of cotransporter function in terms of charge movements associated with presteady-state kinetics is now an established technique and has been applied to a number of Na^+-dependent transporters (e.g., Na^+/Cl^-/GABA transporter, GAT-1 (Mager et al., 1993); isoforms of Na^+/glucose transporters, SGLT-1 (Chen et al., 1996; Hazama et al., 1997; Loo et al., 1993; and Panayotova-Heiermann et al., 1995), Na^+/*myo*-inositol transporter, SMIT (Hager et al., 1995) and Na^+/glutamate transporter, EAAT-2 (Wadiche et al., 1995)). Analysis of charge movements indicated by presteady-state relaxations provides further insights into the individual steps of the transport cycle which are not available from the steady-state analysis alone.

For NaPi-5, we have demonstrated that relaxations can be measured which are directly related to the expression of functional NaPi-5. These relaxations have the properties of intra-membrane charge movements associated with voltage-dependent transitions as indicated by: (i) charge balance on ON and OFF transitions; (ii) reversal at the holding potential; (iii) saturation of the equivalent charge-voltage (*Q-V*) relation and (iv) a relaxation time constant which is dependent on the target potential. That NaPi-5 itself is the source of these relaxations is suggested indirectly by the absence of relaxations in non-injected oocytes, and more directly by the linear correlation between maximum steady-state current at a strongly hyperpolarizing potential ($I_p(-140)$ and $Q_{\max}$ predicted from the Boltzmann fit to the *Q-V* data for different oocytes (Fig. 4*E*).

The slope of the $I_{p\max}/Q_{\max}$ relation can be used to

estimate the equivalent turnover rate for NaPi-5. Here we assume that the charge translocation is a single step having an apparent valence *z* and that the same number of transporters contribute to the maximum steady-state current in the presence of saturating P_i, as contribute to the maximum charge movement (Q_{max}) in the absence of P_i. The transporter turnover, ϕ, is then given by:

$$\phi = I_{p\text{-}max} \cdot z/Q_{max} \quad (4)$$

Taking $z = 0.71$ (Fig. 4*D*) and $I_{pmax}/Q_{max} = 50\ sec^{-1}$ (Fig. 4*E*). Equation 4 gives $\phi = 35\ sec^{-1}$ at −140 mV and 96 mM Na^+. This compares well with estimates of ϕ for other Na^+-coupled transporters expressed in *Xenopus* oocytes at the same Na^+ concentration: (e.g., rat SGLT-1 ($30\ sec^{-1}$), Panayotova-Heiermann et al. (1995); human EEAT-2 ($29\ sec^{-1}$), Wadiche et al., 1995 and canine SMIT ($5–25\ sec^{-1}$), Hager et al., 1995)). It should be noted this represents a lower limit for estimating ϕ because of the assumption that the apparent valence for the single step reaction is *z* and does not take account of multiple subunits, each having a valency *z*, (*see* Zamphigi et al., 1995). Furthermore, this estimate is made at a nonsaturating Na^+ concentration.

Origins of the Relaxations

At the temporal resolution possible with the two electrode voltage clamp, we have shown that the NaP_i-5 voltage-dependent presteady-state kinetics are independent of P_i (Fig. 5*C* and *D*), whereas the relaxation kinetics with varying external Na^+ are strongly voltage-dependent. This Na^+-related voltage dependence is most clearly seen from the negative shift in $V_{0.5}$ for the *Q-V* relation (Fig. 6*C*). At first sight this behavior appears qualitatively consistent with that predicted for a single step reaction for Na^+ binding. In such an ion-well model, the Na^+ binding site lies within the transmembrane field and is accessible from both sides of the membrane but not both simultaneously (e.g., Kimmich, 1990). The simplest form of this model predicts that the forward rate constant is proportional to the Na^+ concentration raised to the power *n*, where *n* is the number of Na^+ ions which simultaneously bind at the site, with an apparent valency *z*. From the Table the results of fitting the τ-*V* data to a single transition Boltzmann function (Eq. 2, Materials and Methods) show that this is clearly not the case, since the zero voltage forward rate constant (A_o) varies only weakly for a 4-fold change in Na^+ concentration, whereas *z* decreases significantly. Moreover, by differentiating Eq. 2 it can be shown that the maximum of the τ-*V* curve, τ_{max} is given by:

$$\tau_{max} = [(1 - \delta)/A_o]^{1-\delta}\ [\delta/B_o]^{\delta} \quad (5)$$

and the maximum occurs at a potential V_{max}:

$$V_{max} = kT/ze\ \ln[\delta A_o/(1 - \delta)B_o)] \quad (6)$$

Thus, for a decrease in external Na^+, Eq. 6 predicts a left shift of the position of the V_{max} as we observe (Fig. 6*B*), and an increase in the maximum time constant, τ_{max} (Eq. 5) which is the opposite of what we observe. This suggests that the observed presteady-state relaxations cannot be explained simply in terms of a single ion well model involving one binding step for Na^+. More complex models could be proposed: for example, the Na^+ binding might involve several kinetic steps which cannot be detected, or Na^+ might bind at several sites as suggested above. Nevertheless, in the context of developing a kinetic model for Na^+/P_i cotransport, the observed Na^+-dependence of the presteady-state relaxations and their presence with 0 mM P_i strongly suggests that in any ordered binding scheme, the first external binding step should involve Na^+.

Our finding that increasing the pH decreases the amount of charge in full Na^+ provides further support for the hypothesis that protons compete for occupancy of the Na^+ binding site(s) (Busch et al., 1994; Murer & Biber, 1996). Furthermore, in agreement with earlier uptake studies (Amstutz et al., 1985), no P_i-induced steady-state transport was measured in the absence of external Na^+ with a >10-fold change in H^+ (pH 7.4 to 6.2). Interestingly, at the time resolution available with the two electrode voltage clamp, under the same superfusion conditions, we also observed no change in the relaxation time course over a wide range of test potentials from pH 7.4 to 6.2. This suggests that protons might not enter the transmembrane electric field, but simply prevent access to the Na^+ binding site through an allosteric mechanism or directly at the point of entry of Na^+ into the transmembrane field. This latter action of protons would add further support to the hypothesis that Na^+ binding involves multiple sites, not all of which lie within the transmembrane field.

Finally, the unloaded carrier itself could be a likely contributor to the total charge movement, since we observed charge movements in the absence of external Na^+. It should be noted however that with the intact oocyte preparation, we cannot exclude the possibility that with 0 mM external Na^+, binding of internal Na^+ could also contribute to the measured charge movements. This could only be tested using the cut-open oocyte technique which, in addition to faster voltage clamping, would allow internal perfusion (e.g., Chen et al., 1996; Taglialatela et al., 1992).

A Simple Kinetic Scheme Accounts Qualitatively for the Voltage Dependence of NaPi-5 Presteady State Relaxations

The above findings have allowed us to identify certain partial reactions in the overall Na^+/P_i cotransport cycle

which form part of a multi-state ordered kinetic scheme as depicted in Fig. 8*A*. This model is similar to the 6-state scheme proposed for the cloned sodium-glucose cotransporter (SGLT-1) (Loo et al., 1993, Hazama et al., 1997; Parent et al., 1992), derived from electrophysiological measurements, but incorporates two Na^+ binding steps as for the ordered terter model developed by Restropo & Kimmich (1985) to describe the sodium-glucose system in chick epithelia. In these models the substrate binding site(s) can be orientated either towards *trans* or *cis* sides of the membrane through reorientation of the carrier. From our findings for substrate NaPi-5 interaction, we assume that on the *cis* side, the first substrate to bind to the unloaded carrier is one Na^+ ion (1⇒2) (*see below*) which then facilitates the P_i binding reaction (2⇒3). The final Na^+ binding reaction (3⇒4), involving two Na^+ ions, takes account of the dependence of $I_{p\,max}$ on Na^+ (Fig. 1*B*) to give an overall net positive charge movement, assuming P_i is transported in its divalent form. The only voltage-dependent transitions arise from the translocation of the unloaded carrier, assumed to be negatively charged, and the first Na^+ binding (6⇒1; 1⇒2). For simplicity, the second Na^+ binding transition (3⇒4) is also assumed voltage independent. This is indirectly supported by our finding that the presteady state kinetics appear to be unaffected by changes in P_i, the presence of which would allow transition 3⇒4 to occur. However, additional experiments would be required to test this assumption more fully, since rapid voltage-dependent transitions could be masked by the limited signal resolution available with the whole oocyte clamp. On the *trans* side, we have arbitrarily lumped the substrate release transitions together (5⇒6) because the intact oocyte preparation does not allow ready modification of internal substrate concentrations to characterize these transitions. Finally, we assume that there is no uncoupled transport (i.e., Na^+ leak), as considered by Wright and colleagues (e.g., Umbach et al., 1990).

To explore the behavior of this model in terms of its ability to account for the presteady state behavior, values for the four voltage dependent rate constants k_{12},k_{21}, k_{61},k_{16}, apparent valencies and asymmetry factors were assigned such that reasonable agreement with the measured τ-*V* and *Q*-*V* data (Fig. 6*B* and *C*) was obtained for two nominal concentrations of Na^+ (96 mM, 25 mM). To account for the change in τ-*V* relation with Na^+ concentration and shift in $V_{0.5}$ of the *Q*-*V* relation, it was sufficient to assume that only one Na^+ ion contributes to the presteady-state relaxations. As noted by Chen et al. (1996) for SGLT-1, it is difficult to distinguish between models with one or two Na^+ ions contributing to the voltage dependence on the basis of the relaxation kinetics alone. Furthermore, good agreement with data was obtained for the apparent valency of the unloaded carrier (0.5) greater than that associated with the Na^+ binding transition (1⇒2) (0.2). The magnitude of this latter parameter suggests that in the *cis* orientation, the binding site is located close to the external membrane surface. Finally, some asymmetry for the energy barrier positions for each transition was assigned to achieve agreement with the measured τ-*V* data.

As shown in Fig. 8*B*, this model predicts presteady-state relaxations having the same form as those measured (compare with Fig. 6*A*) for nominally 96 mM and 25 mM Na^+. As expected for a three state model, two non-zero eigenvalues or exponential components are present, both of which are functions of all 4 rate constants. In our case, the faster relaxation was not measurable with the whole oocyte configuration because it is mixed with the endogenous oocyte capacitive transient and is low-pass filtered by the intrinsic impedance of the oocyte membrane. Moreover, as shown in Fig. 8*C*, its τ-*V* curve is relatively flat over the experimental voltage range. The voltage dependence of the reciprocal rate constants at 96 mM and 25 mM Na^+ is also shown. With respect to the slower time constant, the model predicts the observed shift in V_{max} as well as the decrease in τ_{max} when external Na^+ is reduced. This is seen from the Na^+-dependence of one rate constant, k_{12}: for high Na^+ concentrations, the Na^+ binding transition 1⇒2 is very rapid and the detected exponential will be principally determined by the rate of constants from the unloaded carrier transition 6⇒1. As Na^+ is reduced, k_{12} decreases which causes skewing of the τ-*V* relation and a reduction in τ_{max}. The fast exponential component becomes slower, but still detection of two components in the presteady-state relaxation would be difficult because the separation in τs is too small.

For the corresponding *Q*-*V* curves, shown in Fig. 8*D*, the model predicts the negative shift in $V_{0.5}$ observed (*see* Fig. 6*C*) and a constancy for the apparent valency and Q_{max}. At 96 mM Na^+ the two transitions have similar midpoint voltages and the slope of the total charge curve at the midpoint voltage predicts an apparent valency of 0.6 which agrees with measurement. As Na^+ decreases, the distribution of charge due to Na^+-dependent transition 1⇒2 shifts to the left. This causes a skewing of the overall *Q*-*V* curve which explains the reductions in *z* and Q_{max} in the Table, which were obtained by assuming a single Boltzmann distribution. Note that the charge distributions for both transitions are affected by a change in Na^+ since both are functions of the occupancy of state 2. In practice it would be necessary to fit the *Q*-*V* data to a double Boltzmann distribution to resolve the two apparent valencies, however the lack of saturation at low Na^+ over the workable voltage range and measurement at 20 mV intervals limits the accuracy of the fit (Hazama et al., 1997).

As we have not performed a model optimization, the set of kinetic parameters chosen is not necessarily

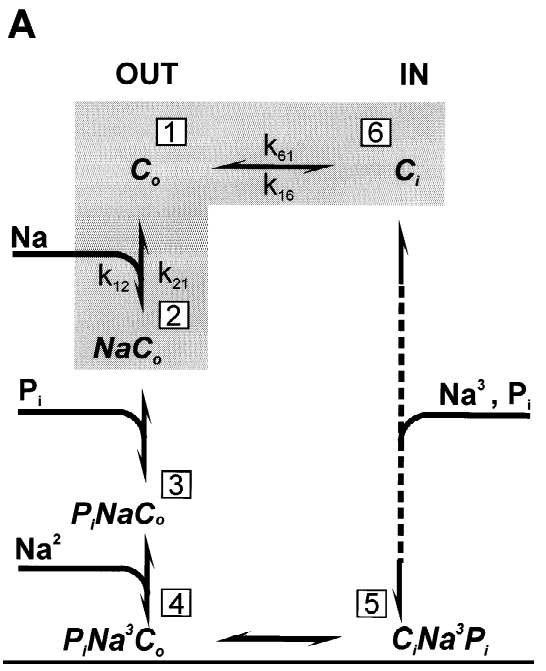

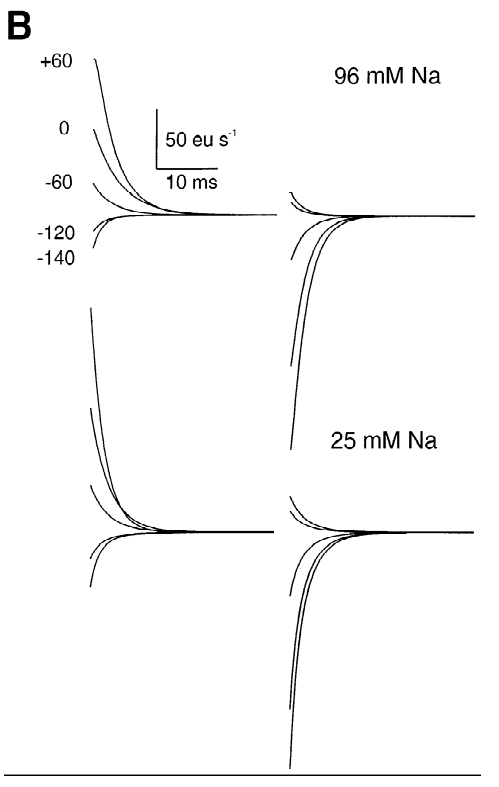

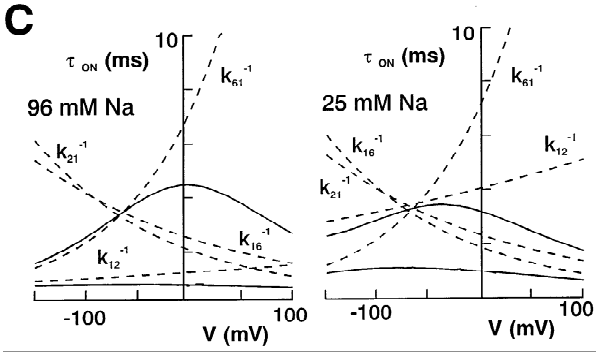

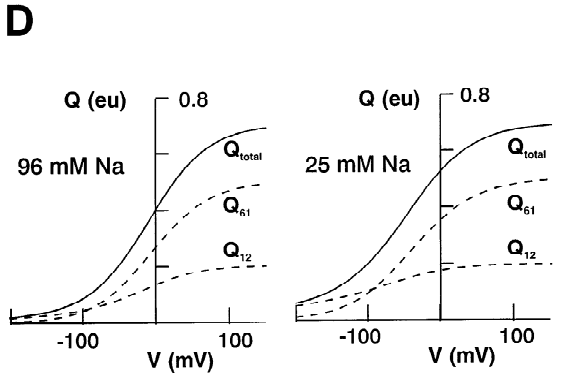

Fig. 8. Modeling the voltage dependent partial reactions of NaPi-5 (*A*) State diagram of 6 state kinetic model for NaPi-5. Voltage-dependent transitions identified by experiments are shown shaded. Under physiological conditions (membrane potential <0) transport proceeds anti-clockwise around the loop. The unloaded carrier can face either the cytosol (C_i: state 6) or external medium (C_o: state 1), but favors the external medium for V <0. Each state is distinguished by the substrate(s) bound and its membrane orientation. One Na^+ ion binds first (transition 1⇒2) followed by P_i (transition 2⇒3) and a second Na^+ binding step involving two Na^+ ions (3⇒4) occurs, whereupon the fully loaded carrier can reorientate to the cytosolic face (transition 4⇒5) and release the bound substrates (lumped as transition 5⇒6). (*B*) Presteady-state currents predicted from model in response to voltage steps indicated from a holding potential of −100 mV with nominal 96 mM Na^+ and 25 mM Na^+. Voltage step is assumed to occur instantaneously—i.e., no account has been taken of the speed of voltage clamp and charging of oocyte membrane. Model parameters, based on trial and error parameter adjustment comparing with data of Fig. 6, are as follows: at $V = 0$, $k_{61} = 140\ sec^{-1}$; $k_{16} = 550\ sec^{-1}$; $k_{12} = 10000\ M^{-1}sec^{-1}$; $k_{21} = 440\ sec^{-1}$ and $z_{61} = 0.5$; $z_{12} = 0.2$; $\delta_{61} = 0.3$. Ordinate scale is in electronic units (eu) sec^{-1}, where $1\ eu = 1.602 \times 10^{-19}\ C$. (*C*) τ-*V* curves for model with same two Na^+ concentrations using parameters given in *B*, showing exponential components which account for the relaxations of *B* (continuous curves). The 3-state model predicts two time constants: the faster one would not be easily detectable using a two-electrode voltage clamp, but may influence the fitting procedure. The voltage-dependence of the reciprocal rate constants is also shown (dashed curves) of which k_{12}^{-1} is the only reciprocal rate constant dependent on Na^+. (*D*) *Q*-*V* curves for model with same two Na^+ concentrations. Steady-state charge distribution for total charge transfer (in eu's) is shown by continuous lines; charge distributions for the individual steps (transitions 6⇒1; 1⇒2) are shown dashed.

unique, nevertheless we are able to account qualitatively for the voltage dependence of the presteady-state behavior observed over a fourfold change in Na^+ concentration. It should therefore serve as a basis for future modeling studies with the availability of more precise data and, moreover, be able to predict the steady-state behavior. The presteady-state relaxations we have measured from NaPi-5 expressing oocytes are approximately threefold faster than those reported for SGLT1 (Loo et al., 1993). This represents the lower limit of time domain resolution possible with the two electrode voltage clamp applied to an intact oocyte because of the bandwidth limitations imposed by the intrinsic oocyte impedance. It also explains why we were only able to detect one exponential component in the relaxations with confidence. To improve the signal resolution necessary for more advanced modeling of NaPi-5, the cut-open oocyte technique will be required to provide improvement in bandwidth and voltage clamping speed (Chen et al., 1996; Taglialatela et al., 1992).

The kinetic behavior we report here for the flounder type II Na^+/P_i cotransporter NaPi-5, is consistent with that for other Na^+-dependent cotransporters. Our findings suggest that, despite the lack of structural homology between type II Na^+/P_i cotransporters and members of the Na^+/glucose, Na^+/neurotransmitter families (Wright et al., 1996), a common mechanism of action is shared by many electrogenic cation-coupled cotransporters.

We thank Dr. D.D.F. Loo, Dr. F. Verrey and Prof. E.M. Wright for helpful comments and critical reading of the manuscript. A.E.B. is a Heisenberg Fellow. The work was supported by grants to H.M. from the Swiss National Science Foundation (SNF: 31-46523), the Hartmann Müller-Stiftung (Zurich), the Olgar Mayenfisch-Stiftung (Zurich) and the Schweizerischer Bankgesellschaft (Zurich) and to A.E.B. from the Deutsche Forschungsgemeinschaft (Bu 704/7-1).

References

Amstutz, M., Mohrmann, M., Gmaj, P., Murer, H. 1985. Effect of pH on phosphate transport in rat renal brush border vesicles. *Am. J. Physiol.* **248:**F705–710

Berndt, T.J., Knox, F.G. 1992. Renal regulation. *In:* The Kidney: Physiology and Pathophysiology. D.W. Seldin and G. Giebisch, editors. pp. 2511–2532. Raven Press, New York

Bertrand, D., Bader, Ch. 1986. DATAC: a multipurpose biological data analysis program based on a mathematical interpreter. *Int. J. Bio-Med. Comput.* **18:**193–202

Biber, J., Custer, M., Magagnin, S., Hayes, G., Werner, A., Lötscher, M., Kaissling, B., Murer, H. 1996. Renal Na/Pi-cotransporters. *Kidney Int.* **49:**981–985

Boorer, K.J., Loo, D.D.F., Wright, E.M. 1994. Steady-steady state and presteady-state kinetics of the H^+/hexose cotransporter (STP1) from *Arabidopsis thalania* expressed in *Xenopus* oocytes. *J. Biol. Chem.* **269:**20417–20424

Boorer, K.J., Loo, D.D.F., Frommer, W.B., Wright, E.M. 1996. Transport mechanism of the cloned potato H^+/sucrose cotransporter StUT1. *J. Biol. Chem.* **271:**25139–25144

Busch, A.E., Kavanuagh, M.P., Varnum, M.D., Adelman, J.P., North, R.A. 1992. Regulation by second messengers of the slowly-activating, voltage-dependent potassium current in *Xenopus* oocytes. *J. Physiol.* **450:**455–468

Busch, A.E., Waldegger, S., Herzer, T., Biber, J., Markovich, D., Hayes, G., Murer, H., Lang, F. 1994. Electrophysiological analysis of Na^+/P_i cotransport mediated by a transporter cloned from rat kidney in *Xenopus* oocytes. *Proc. Natl. Acad. Sci. USA* **91:**8205–8208

Busch, A.E., Wagner, C.A., Schuster, A., Waldegger, S., Biber, J., Murer, H., Lang, F. 1995. Properties of electrogenic P_i transport by NaPi-3, a human renal brush border Na^+/P_i transporter. *J. Am. Soc. Nephrol.* **6:**1547–1551

Chen, X.Z., Coady, M.J., Lapointe, J-Y. 1996. Fast voltage clamp discloses a new component of presteady-state currents from the Na^+-glucose cotransporter. *Biophys. J.* **71:**2544–2552

Forster, I., Busch, A.E., Lang, F., Biber, J., Murer, H. 1996. Pre-steady-state relaxations exhibited by the rat renal type II Na/P_i cotransporter (NaPi-2) expressed in *Xenopus* oocytes. *J. Am. Soc. Nephrol.* **7:** Abstract A2770, ASN Meeting 1996

Gupta, A., Renfro, J.L. 1991. Effects of pH on phosphate transport by flounder renal tubule primary cultures. *Am. J. Physiol.* **260:**R704–711

Hager, K., Hazama, A., Kwon, H.M., Loo, D.D.F., Handler, J.S., Wright, E.M. 1995. Kinetics and specificity of the renal Na^+/*myo*-inositol cotransporter expressed in *Xenopus* oocytes. *J. Membrane Biol.* **143:**103–113

Hartmann, C.M., Wagner, C.A., Busch, A.E., Markovich, D., Biber, J., Lang, F., Murer, H. 1995. Transport characteristics of a murine renal Na/P_i-cotransporter. *Pfluegers Arch.* **430:**830–836

Hazama, A., Loo, D.D.F., Wright, E.M. 1997. Presteady-state currents of the Na^+/glucose cotransporter (SGLT1). *J. Membrane Biol.* **155:**175–186

Hoffmann, N., Thees, M., Kinne, R. 1976. Phosphate transport by isolated renal bush border vesicles. *Pfluegers Arch.* **362:**147–156

Jack, J.J.B., Nobel, D., Tsien, R.W. 1983. Electric current flow in excitable cells. Oxford University Press, Oxford

Kimmich, G.A. 1990. Membrane potentials and the mechanism of intestinal Na^+-dependent sugar transport. *J. Membrane Biol.* **114:**1–27

Klamo, E.M., Drew, M.E., Landfear, S.M., Kavanaugh, M.P. 1996. Kinetics and stoichiometry of a proton/*myo*-inositol cotransporter. *J. Biol. Chem.* **271:**14937–14943

Kohl, B., Herter, P., Huelseweh, B., Elger, M., Hentschel, H., Kinne, R.H., Werner, A. 1996. Na-P_i cotransport in flounder: same transport system in kidney and intestine. *Am. J. Physiol.* **270:**7–944

Loo, D.F., Hazama, A., Supplisson, S., Turk, E., Wright, E.M. 1993. Relaxation kinetics of the Na^+/glucose cotransporter. *Proc. Nat. Acad. Sci.* **90:**5767–5771

Mager, S., Naeve, J., Quick, M., Labarca C., Davidson, N., Lester, H.A. 1993. Steady states, charge movements, and rates for a clones GABA transporter expressed in *Xenopus* oocytes. *Neuron* **10:**177–188

Murer, H., Biber, J. 1992. Renal tubular phosphate transport. Cellular mechanisms. *In:* The Kidney. Physiology and Pathophysiology. 2nd ed., D.W. Seldin and G. Giebisch, editors. pp. 2481–2509. Raven Press, New York

Murer, H., Biber, J. 1996. Molecular mechanisms of renal apical Na phosphate cotransport. *Ann. Rev. Physiol.* **58:**607–618

Panayotova-Heiermann, M., Loo, D.D.F., Wright, E.M. 1995. Kinetics of steady-state currents and charge movements associated with the rat Na^+/glucose cotransporter. *J. Biol. Chem.* **270:**27099–27105

Parent, L., Supplisson, S., Loo, D.D.F., Wright, E.M. 1992. Electrogenic properties of the cloned Na^+/Glucose cotransporter: II A

transport model under nonrapid equilibrium conditions. *J. Membrane Biol.* **125:**63–79

Press, W.H., Flannery, B.P., Teukolsky, S.A., Vetterling, W.T. 1992. Numerical recipes in C. Cambridge Univ. Press, Cambridge

Renfro, J.L., Gupta, A. 1990. Comparative physiology of phosphate transport across renal plasma membranes. *In:* Comparative Aspects of Sodium Cotransport Systems. R.K.H. Kinne, editor. pp. 216–240. Karger, Basel

Restrepo, D., Kimmich, G.A. 1985. Kinetic analysis of mechanism of intestinal Na^+-dependent sugar transport. *Am. J. Physiol.* **248:**C498–C509

Stein, W.D. 1990. Channels, carriers and pumps. Academic Press, San Diego

Taglialatela, M., Toro, L., Stefani, E. 1992. Novel voltage clamp to record small, fast currents from ion channels expressed in *Xenopus* oocytes. *Biophys. J.* **61:**78–82

Umbach, J.A., Coady, M.J., Wright, E.M. 1990. Intestinal Na^+/glucose cotransporter expressed in *Xenopus* oocytes is electrogenic. *Biophys. J.* **57:**1217–1224

Wadiche, J.I., Arriza, J.L., Amara, S.G., Kavanaugh, M.P. 1995. Kinetics of a human glutamate transporter. *Neuron* **14:**1019–1027

Werner, A., Murer, H., Kinne, R.K.H. 1994. Cloning and expression of a renal Na-P_i cotransport system from flounder. *Am. J. Physiol.* **267:**F311–317

Wright, E.M., Loo, D.D.F., Turk, E., Hirayama, B.A. 1996. Sodium cotransporters. *Current Opin. in Cell Biol.* **8:**468–473

Zamphigi, G.A., Kreman, M., Boorer, K.J., Loo, D.D.F., Benzanilla, F., Chandy, G., Hall, J.E., Wright, E.M. 1995. A method for determining the unitary functional capacity of cloned channels and transporters expressed in *Xenopus laevis* oocytes. *J. Membrane Biol.* **148:**65–78